Available online at www.sciencedirect.com
SCIENCE DIRECT
Journal of Power Sources 157 (2006) 226–243
JOURNAL OF POWER SOURCES
www.elsevier.com/locate/jpowsour

Liquid water transport in straight micro-parallel-channels with manifolds for PEM fuel cell cathode

Kui Jiao, Biao Zhou *, Peng Quan

Department of Mechanical, Automotive & Materials Engineering, University of Windsor, Ont., Canada N9B 3P4

Received 8 May 2005; accepted 2 June 2005
Available online 23 March 2006

Abstract

Water management in a proton exchange membrane (PEM) fuel cell stack has been a challenging issue on the road to commercialization. This paper presents a numerical investigation of air–water flow in micro-parallel-channels with PEM fuel cell stack inlet and outlet manifolds for the cathode, using a commercial Computational Fluid Dynamics (CFD) software package FLUENT. Different air–water flow behaviours inside the straight micro-parallel-channels with inlet and outlet manifolds were simulated and discussed. The results showed that excessive and unevenly distributed water in different single PEM fuel cells could cause blockage of airflow or uneven distribution of air along the different flow channels. It is found that for a design with straight-channels, water in the outflow manifold could be easily blocked by air/water streams from the gas flow channels; the airflow could be severely blocked even if there was only a small amount of water in the gas flow channels. Some important suggestions were made to achieve a better design.

Keywords: Water management; PEM fuel cell stack; Air–water behaviour; CFD modeling; FLUENT

1. Introduction

Low operating temperature and zero/low emissions have made polymer electrolyte membrane (PEM) fuel cells become the most promising power source for vehicle and portable applications of the future [1]. However, to achieve commercialization, the performance of PEM fuel cells needs to be improved by proper engineering design and optimization. Due to the special chemical structure of the PEM, the membrane must be well hydrated to ensure that a sufficient amount of hydrogen ions could cross. On the other hand, due to the low operating temperature of PEM fuel cells (30–100 °C) [1], excessive humidification could result in water vapour condensation that could subsequently block the gas flow channels resulting in a lower airflow rate on the cathode side, thus decreasing fuel cell performance. Water content is also an important factor that affects the ohmic resistance in the membrane [2]. Therefore, keeping an appropriate amount of water content in the fuel cell to avoid both membrane dehydration and water vapour condensation has been a critical issue in improving fuel cell performance. In reality, however, attempting to satisfy water management on both the anode and cathode sides without dehydration and condensation is hard to achieve. In other words, water vapour condensation in the gas flow channels of practical fuel cell application is unavoidable [2]. Therefore, water management has been a critical issue for high performance fuel cell design and optimization, and recently many engineers and scientists have paid particular attention to it.

In the last decades, water management related studies were performed numerically and experimentally for different purposes and in several ways. A three-dimensional numerical simulation of a straight gas flow channel in a PEM fuel cell was performed by Dutta et al. [3] using a commercial Computational Fluid Dynamics (CFD) software FLUENT. They found that membrane thickness, cell voltage and current density could affect water transport across the membrane. Hontanon et al. [4] also employed FLUENT to implement their 3D, stationary gas flow model. However, both references [3,4] neglected the effects of liquid water during their simulations. Yi et al. [2] pointed out that water vapour condensation was inevitable on both the anode and cathode sides of a PEM fuel cell, and they discussed a liquid water removal technique that used a water transport plate to

* Corresponding author. Tel.: +1 519 253 3000x2630.
E-mail address: bzhou@uwindsor.ca (B. Zhou).

0378-7753/$ – see front matter © 2006 Published by Elsevier B.V.
doi:10.1016/j.jpowsour.2005.06.041

Table 1
Six simulation cases for different PEM fuel cell operating conditions

Case no.	Inlet velocity ($m\,s^{-1}$)	Initial water (mm^3)	Initial water distribution	Corresponding PEM fuel cell stack operating condition
1	5	3.925	Five spherical droplets ($r=0.5$ mm) freely suspended along the central line of the inlet manifold	Fundamental study of water droplet deformation inside gas flow channels
2	5	50	A water film with a thickness of 0.5 mm placed on the bottom surface of the inlet manifold, with the inlet of each unit cell blocked	Liquid water carried in by air supply covering the bottom surface of the inlet manifold
3	5	42.5	A water film with a thickness of 0.5 mm placed on the bottom surface of the inlet manifold, without the inlet of each unit cell blocked	Liquid water carried in by air supply covering the bottom surface of the inlet manifold
4	5	30	Water films with a thickness of 0.2 mm placed on the leeward (right) side surface of each gas flow channel in the unit cells	Most of the liquid water generated on the leeward side surface of each unit cell gas flow channel
5	5	30	Water films with a thickness of 0.2 mm placed on the windward (left) side surface of each gas flow channel in the unit cells	Most of the liquid water generated on the windward side surface of each unit cell gas flow channel
6	5	45	Water films with a thickness of 0.5 mm attached to surrounding walls near the manifold inlet	Excessive liquid water condensed on manifold inlet surface

lead excess liquid water to the coolant flow channels by a pressure difference. A study exploring the steady-state gas transport phenomena in micro-scale parallel flow channels was conducted by Cha et al. [5]. Oxygen concentration along a single gas flow channel and other flow patterns that may affect fuel cell performance were discussed [5]. Similarly, gas concentration of a steady-state flow along fuel cell flow channels were obtained numerically by Kulikovsky [6]. You and Liu [7] considered liquid water concentration in a straight-channel on the cathode side and concluded that a multi-phase model must be employed to obtain a more realistic simulation result.

By far, most numerical simulation models have focused on a unit cell or simplified stack. Fuel cell stacks with inlet and outlet manifolds are rarely discussed. In addition, flow behaviour of unsteady, two-phase flow in a fuel cell stack with inlet and outlet manifolds is much different from that in a single straight gas flow channel in steady state. Also, there is no literature available to address the liquid water behaviour in fuel cell channels except for the present authors' previous researches [8,9] that dealt with serpentine channels or a single U-shaped channel.

In [8,9], the U-shaped or serpentine channels were investigated. Although the serpentine channels have been regarded as a better design for PEM fuel cell flow channel applications, in reality, there are many cases where the straight-channel design have been utilized for simplicity. But the behaviours of liquid water in straight micro-channels would be different than those in serpentine channels. Therefore in this paper, a fuel cell stack consisting of five unit cells (each with three straight micro-parallel-channels) with inlet and outlet manifolds is proposed to investigate the details of fluid flows and predict the distribution of liquid water in such straight-channel design. The simulation tool employed was the commercial Computational Fluid Dynamics software package FLUENT. In this work, the details of phase change, electro-chemical reaction were not considered here. By considering different initial liquid water distributions, various operating conditions for a fuel cell stack could be simulated.

In the following, the computation domain, the solution procedure and mesh independency are introduced. Then, the results from the six cases (shown in Table 1) with different initial water distributions corresponding to different PEM fuel cell operating conditions are presented. Finally, conclusions are drawn and some valuable design and optimization related suggestions are given.

2. Numerical model setup

2.1. Computation domain and boundary conditions

Fig. 1 illustrates a schematic of the computation domain showing the cathode side of the five-cell PEM fuel cell stack considered with the inlet and outlet flow manifolds at the top and bottom, respectively. The direction of the outlet manifold

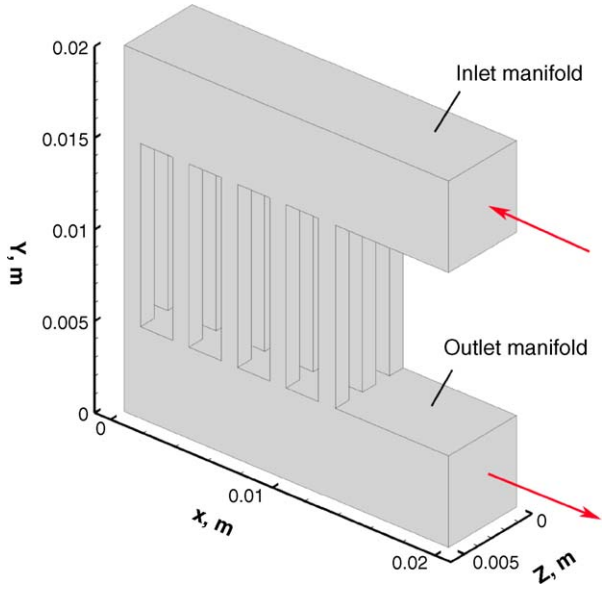

Fig. 1. Computation domain with inlet and outlet manifolds.

was placed which is opposed from normal arrangements, this is because we want to find the problems that could happen in such arrangement. Both manifolds were 20 mm long and had a cross-section of 5 mm × 5 mm with five unit cells connected between them. Each unit cell had three straight parallel gas flow channels 10 mm in height and a cross-section of 1 mm × 1 mm. The isothermal air–water transport process inside the computation domain was modeled as a 3D viscous laminar flow. A no-slip boundary condition was applied to the surrounding walls. A velocity inlet boundary condition (uniform air velocity distribution of 5 m s^{-1} with a direction normal to the inlet boundary) was applied at the air inlet of the inlet flow manifold. At the outlet, the boundary condition was assigned as outlet flow (the gradients of all flow properties are zero). Gravity was taken as being along the negative y-direction. To simulate liquid water behaviour under various PEM fuel cell operating conditions, the initial water distribution inside the computation domain was carefully setup and the details are given in Section 3.

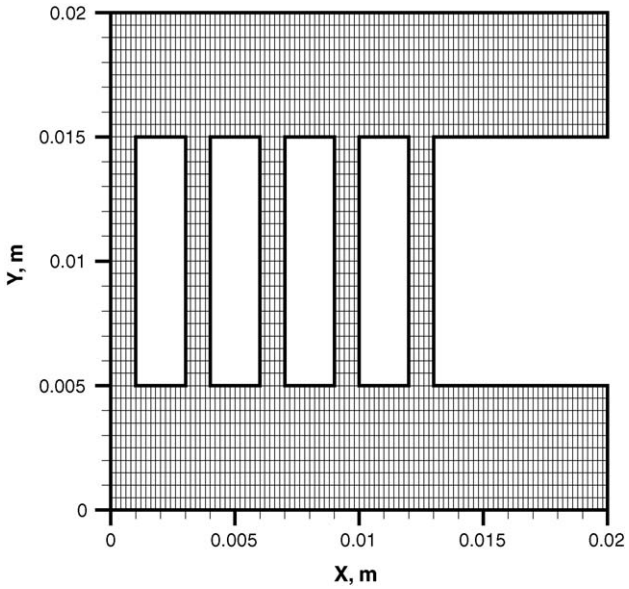

Fig. 2. Mesh on x–y plane.

2.2. Computational methodology

The numerical simulations of the 3D, unsteady, laminar, multi-phase flow in the computation domain was performed using FLUENT. An inspection of the numerical setup revealed that the Reynolds number in the model was less than 1750, thereby supporting laminar flow assumption. No energy equations were considered therefore the conservation of mass and momentum were the governing equations for the model. To track the air–water two-phase flow interface inside the computation domain, the volume-of-fluid (VOF) [10] method implemented in FLUENT was used. The VOF model is designed for two or more immiscible fluids.

Then, the conservation law of mass and momentum governing unsteady, laminar flow could be written as

Continuity equation:

$$\frac{\partial \rho}{\partial t} + \nabla \cdot (\rho \vec{v}) = 0 \tag{1}$$

Momentum equation:

$$\frac{\partial (\rho \vec{v})}{\partial t} + \nabla \cdot (\rho \vec{v} \vec{v}) = -\nabla p + \nabla \cdot (\bar{\bar{\tau}}) + \rho \vec{g} + \vec{F} \tag{2}$$

where p is the static pressure, $\vec{F}$ the momentum source term due to surface tension and $\bar{\bar{\tau}}$ is the stress tensor, which is given by:

$$\bar{\bar{\tau}} = \mu \left[(\nabla \vec{v} + \nabla \vec{v}^{\mathrm{T}}) - \frac{2}{3} \nabla \cdot \vec{v} I \right] \tag{3}$$

where I is the unit tensor.

Volume fraction of liquid water (α_2) could be solved:

$$\frac{\partial \alpha_2}{\partial t} + \vec{v} \cdot \nabla \alpha_2 = 0 \tag{4}$$

Then, the volume fraction of air (α_1) could be calculated by using the relation:

$$\alpha_1 + \alpha_2 = 1 \tag{5}$$

All the other properties (e.g., viscosity) could be computed in a volume-fraction weighted-average manner as:

$$\mu = \alpha_2 \mu_2 + (1 - \alpha_2) \mu_1 \tag{6}$$

The effects of surface tension along the interface between each pair of phases and wall adhesion play an important role in the two-phase flow process in the micro-channel and it could be included in the VOF model [10]. In the present work, a widely used surface tension model, the continuum surface force (CSF) model proposed by Brackbill et al. [11] was adopted. With this model, the consideration of surface tension results in a source term, $\vec{F}$ in the momentum Eq. (2). Additionally, effects of wall adhesion were taken into account by specifying a wall adhesion angle in conjunction with the CSF model in the FLUENT throughout the simulation.

2.3. Validation of grid independency

There were 65,000 cells meshed in the computation domain. Fig. 2 shows the mesh on the x–y plane. Each cell had the same size with dimensions 0.2 mm × 0.5 mm × 0.2 mm (along x-, y- and z-directions, respectively). Grid independency was tested by increasing and decreasing the number of grid cells by 20 and 50% for both with small and large amounts of water (Cases 1 and 2, as shown in Table 1). The flow phenomena of liquid water and the velocity field were almost the same. The difference in results for the different mesh systems is so small that it is negligible. Therefore, the general transport of water inside the gas flow channels, with sufficient mesh, can be obtained accurately and efficiently.

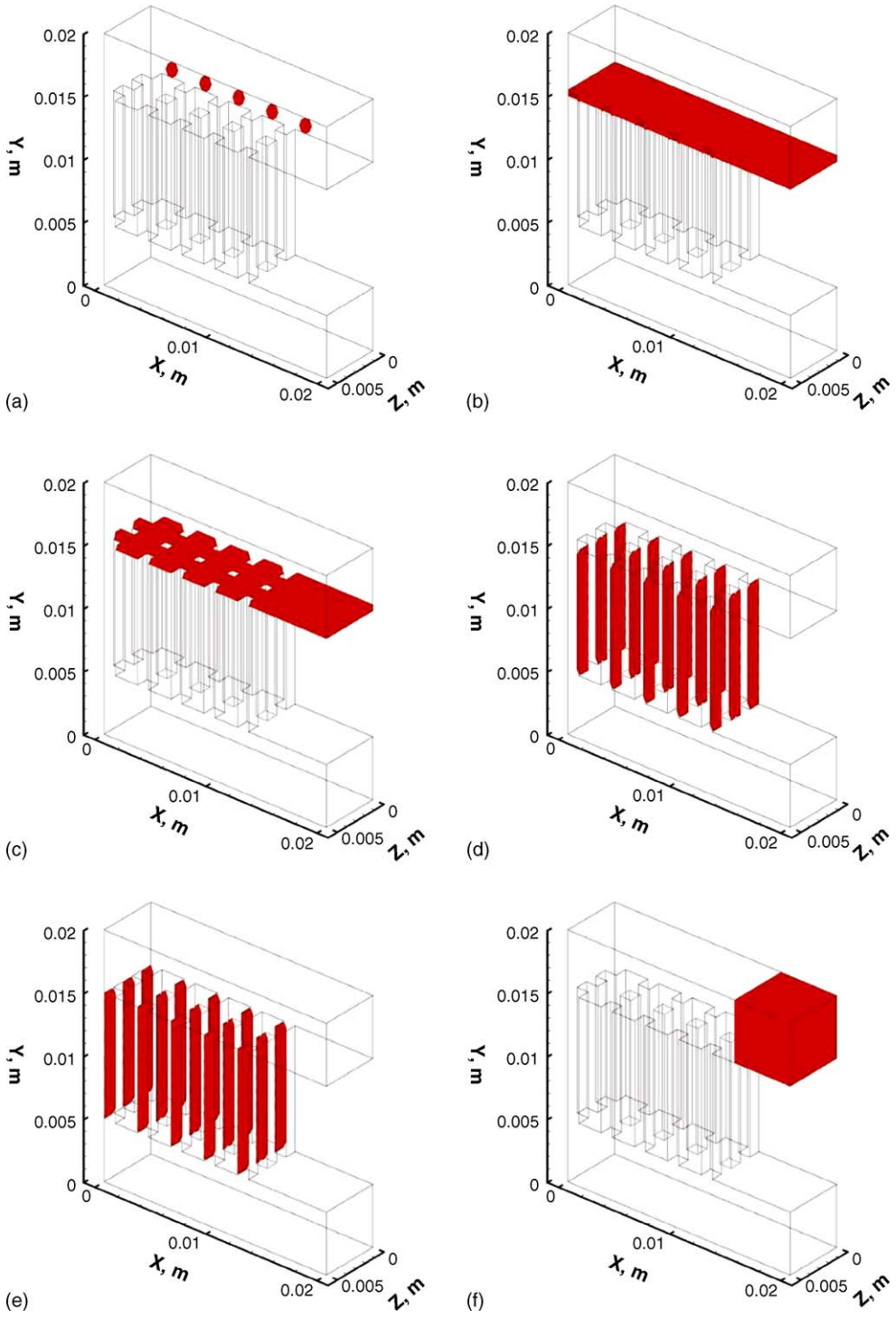

Fig. 3. Initial water distribution for six simulation cases: (a) Case 1; (b) Case 2; (c) Case 3; (d) Case 4; (e) Case 5; (f) Case 6.

3. Results and discussions

In order to investigate two-phase flow behaviour inside the five-cell stack with manifolds, six different cases corresponding to six different PEM fuel cell stack operating conditions were simulated, as listed in Table 1 and shown in Fig. 3. Detailed results and discussions are given as follows.

3.1. Case 1: five spherical droplets freely suspended in the inlet manifold

In Case 1, as a basis, behaviour of small water droplets inside the gas flow channels was studied. Five water droplets were placed in the inlet flow manifold as shown in Fig. 3(a). Each single droplet had a radius of 0.5 mm and the droplet centers were along the centerline of the inlet manifold and evenly distributed.

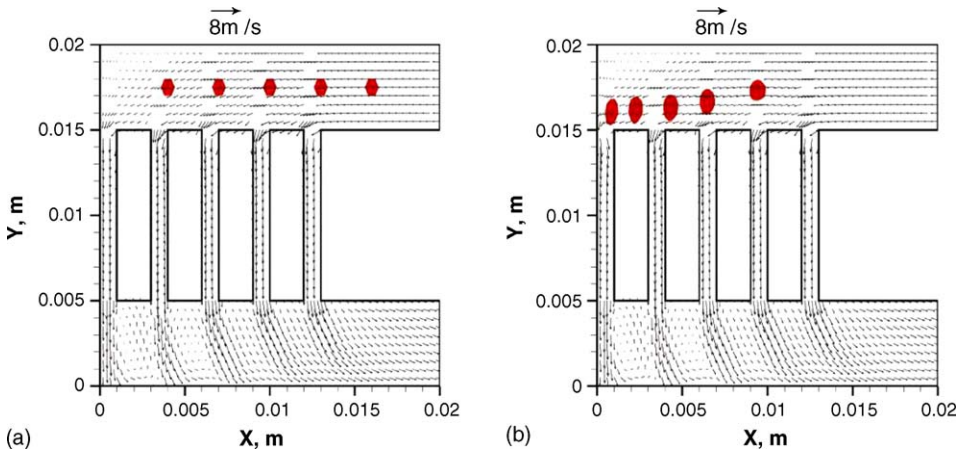

Fig. 4. Water droplet deformation and velocity field on the center-plane of the z-direction ($z = 2.5$ mm): (a) $t = 0$ ms and (b) $t = 1.5$ ms.

The interaction between water and airflow, and the velocity field variation of airflow around liquid water were investigated.

3.1.1. Deformation of water droplets

Fig. 4 shows water droplet behaviour versus time as the droplets travelled through the inlet manifold on the center-plane of the z-direction. Initially, five freely suspended droplets, with their original spherical shape, were placed in the inlet manifold. Subsequently, droplet deformation along the negative x- and y-directions, attributable to effects of both a dragging force from the airflow and gravity, could be noticed. The droplet on the far right section had the largest deformation along the negative x-direction, and did not elongate along the y-direction significantly. However, the droplet on the far left section had its largest deformation along the negative y-direction. Because airflow originated at the inlet, the interaction between airflow and the water droplets was significant for the droplet on the far right section. With an increase of water droplet surface area along the x-direction, a force balance could be achieved and prevent this droplet from moving down due to gravity. Furthermore, the droplet on the far right section blocked some of the airflow resulting in reduced airflow effects on the other droplets. In other words, shear stress would keep decreasing along the main flow direction and correspondingly, the effect of gravity on the left side droplets would become more significant than the right side. This is the reason why the far left droplet had its largest deformation along the negative y-direction and no significant deformation along the x-direction. Therefore, it could be concluded that the droplet closest to the air inlet suffered the largest air dragging forces while gravity effects were insignificant compared to the inertia forces and thus only a slight displacement along the negative y-direction occurred.

3.1.2. General movement of water

When the water droplets approached the wall, at $x = 0$, the velocity field at the near-wall surfaces would change with liquid water displacement. Fig. 5 shows how the velocity field was affected by liquid water displacement on the plane close to $x = 0$. It also shows that airflow was deflected at the near-wall surfaces. In the upper part of the cross-section, airflow was directed upward (along the positive y-direction). With water approaching the surface, the original upward velocity increased due to the squeeze effect between the wall and the water droplets. The squeeze effect would also force the velocity field to expand horizontally (along the z-direction) and hence force all the liquid water to expand to both sides along the z-direction. Simultaneously, water would be divided into two parts: most of the water would descend (along the negative y-direction) into the far left gas flow channels, while the rest would ascend due to the upward airflow. As shown in Fig. 6, there is almost no water travelled through the four right unit cells, so the water is not evenly distributed at all. The ascending water will move onto the sidewalls first, and then to the top of the inlet manifold. This part of water was flown away while it almost approached the air inlet. Therefore, the gas flow channels would have some water flowing through them again, but a very small amount.

3.1.3. Sensitivities of flow channels

As was mentioned previously, it could, therefore, be concluded that for this kind of fuel cell stack, it is very difficult to have liquid water distributed evenly along all of the gas flow channels. Fig. 7 shows how air mass flow rate changed in the five unit cells. The cell furthest from the air inlet is cell #1, while the one in the far right cell is cell #5. Cross-sections at $y = 10$ mm were cut through all of the cells, and the mass flow rates of air through these cross-sections at different times were investigated. It is clear that cell #1 was the first cell to have a large reduction in air mass flow rate. This is because almost all the liquid water moved into this cell. Therefore, it can be approved that, once the supplied water moves to one cell, most of the air would pass through the other cells, thus decreasing fuel cell performance. After that, the four left cells would also have airflow reduction while water passed through them, but it has been shown that there is only a very small amount of water passed through the four left cells. Therefore, the results also approved that the air mass flow rate in the gas flow channels is very sensitive as water goes through it, even to very small amounts.

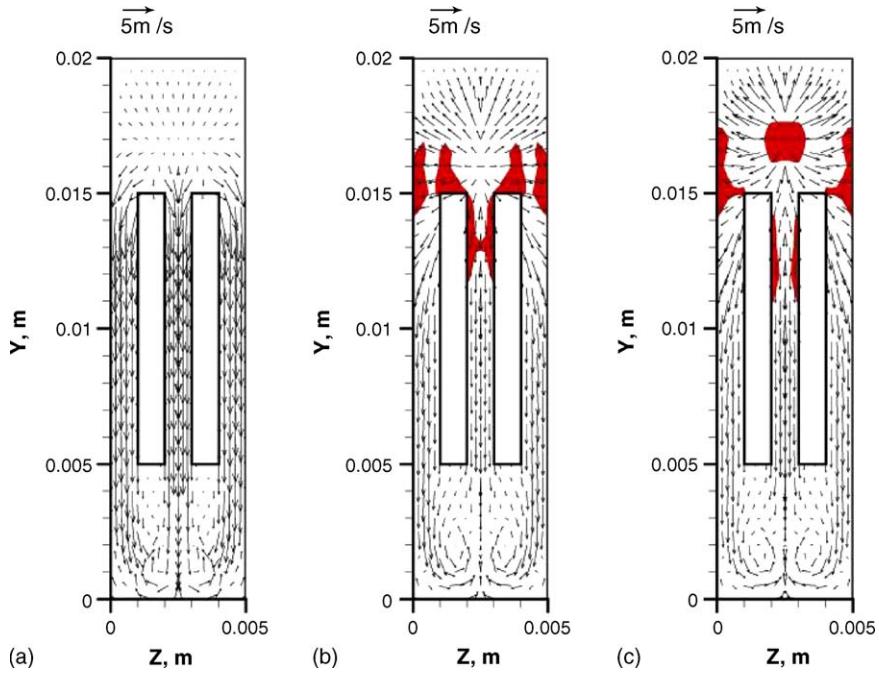

Fig. 5. Velocity field and water distribution on the plane near the wall at $x = 0$: (a) $t = 0$ ms; (b) $t = 3$ ms; (c) $t = 3.3$ ms.

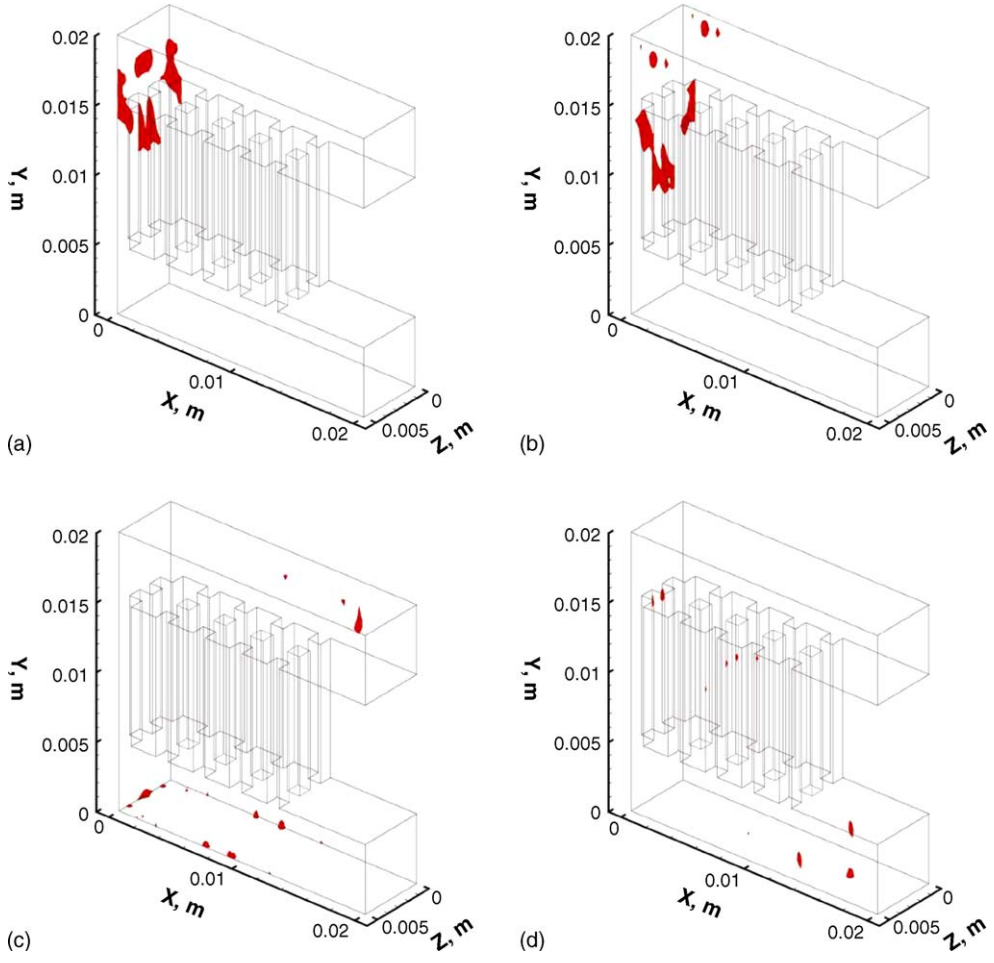

Fig. 6. Water distribution in 3D view at different times: (a) $t = 3.3$ ms; (b) $t = 4.5$ ms; (c) $t = 15$ ms; (d) $t = 30$ ms.

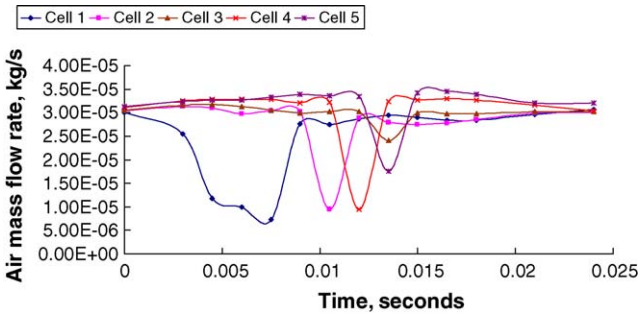

Fig. 7. Air mass flow rate in different cell.

3.1.4. Comparison of water flow in manifolds for both straight and serpentine cell stacks

A straight manifold is usually adopted in fuel cell applications. In reference [9], water flow inside a fuel cell stack was also considered with similar straight manifolds. The water droplet deformation is very similar to the work presented here. The water "flowing backward" phenomenon was also observed in reference [9]. Evenly distributed water was not easy to be obtained if water was supplied in the inlet manifold. Similar to reference [9], in this paper, most of water in the inlet manifold moved into the gas flow channels, which connected the end wall. Therefore, for this kind of parallel gas flow channels, even distribution of water from inlet manifold to the gas flow channels is hard to be achieved.

3.2. Case 2: a water film with a thickness of 0.5 mm placed on the bottom surface of the inlet manifold, with the inlet of each unit cell blocked by the water film

In Case 2, simulation of a large amount of water (due to water addition, condensation and chemical reaction) blocking the inlet of each unit cell was conducted. As shown in Fig. 3(b), a liquid water film with a thickness of 0.5 mm was placed on the bottom surface of the inlet manifold. Differing from Case 1, in this case the inlet of each gas flow channel would be blocked with the same water film, and thus their ability to drain water was tested.

3.2.1. Breaking up of water films and general movement of large amount of water

Fig. 8 shows the water distribution and velocity fields in different views. In Fig. 8(b), water was almost evenly distributed along every gas flow channel at $t = 0.3$ ms, indicating that the velocity fields were very similar along the gas flow channels. Eventually, as shown in Fig. 8(c and d), with different amounts

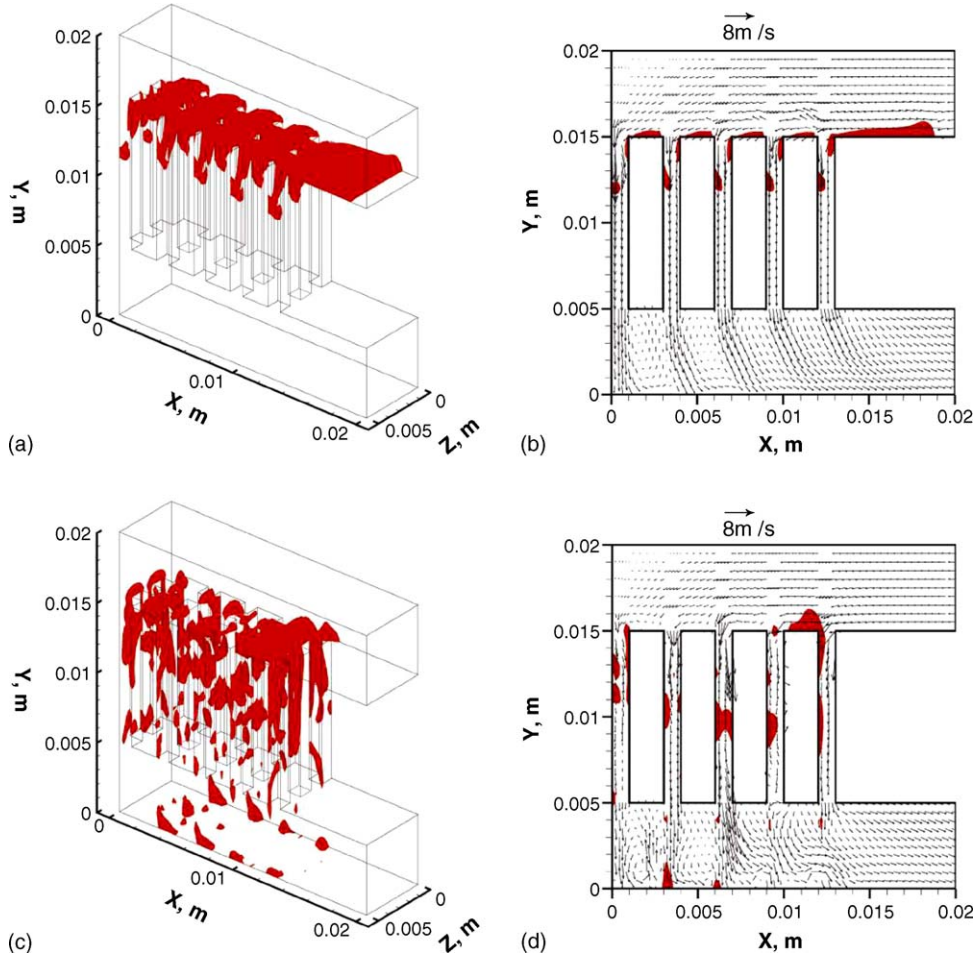

Fig. 8. Water distribution and velocity field in 3D view and on the center-plane of the z-direction: (a) $t = 0.3$ ms, 3D view; (b) $t = 0.3$ ms, on the center-plane of the z-direction ($z = 2.5$ mm); (c) $t = 1.5$ ms, in 3D view; (d) $t = 1.5$ ms, on the center-plane of the z-direction ($z = 2.5$ mm).

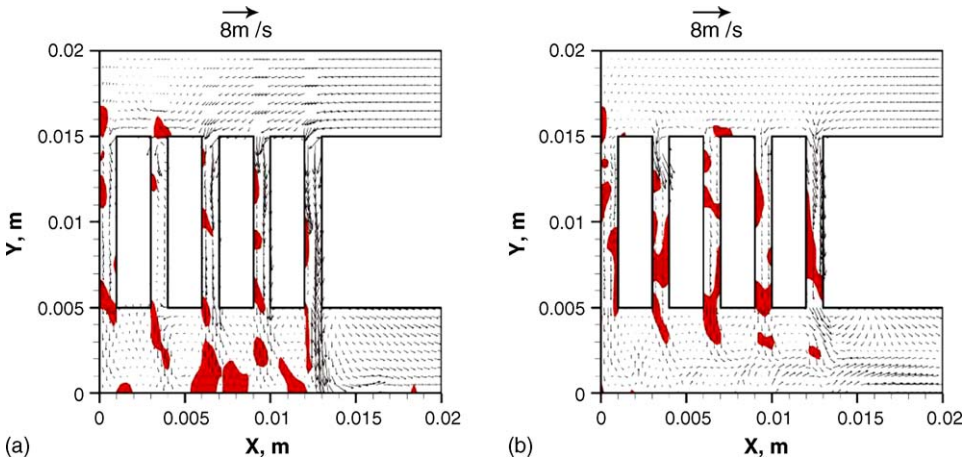

Fig. 9. Water distribution and velocity field on different planes at $t = 3$ ms: (a) $t = 3$ ms, on the center-plane of the z-direction ($z = 2.5$ mm) and (b) $t = 3$ ms, on the plane close to $z = 0$.

of water flowing into different gas flow channels, the water distribution differed. Therefore, the velocity fields along the gas flow channels became very complex and changed dramatically with water flow. There was part of the initial water film, close to each channel inlet, which was slightly hauled up due to the effect of dragging and lifting forces from the airflow, as shown in Fig. 8. Because this part of the water film was lifted up, and all the gas flow channels were filled with water, this part of the water could pass over the inlet of each gas flow channel without sinking in. As shown in Fig. 9, at $t = 3$ ms, most of the air was flowing through the channels furthest away from the hauled up portion of water. This is another reason why water could keep moving forward in the inlet manifold without sinking into the gas flow channels. This part of the water would finally hit the wall at $x = 0$.

After that, Fig. 10 shows a very similar condition to Case 1, in which the far left unit cell was filled with the largest amount of water and thus became blocked. Therefore, air would mainly flow through the channels on the right side. Simultaneously, there was a portion of the water that flowed back to the air inlet. The left side gas flow channels would always have a larger amount of water distribution than the right. Therefore, the right side gas flow channels would always have a stronger air stream flow directed towards the outflow manifold. These air streams could block liquid water flowing through the outflow manifold. In other words, liquid water in the outflow manifold on the left side would have difficulty flowing out hence this part of the water would ascend (along the positive y-direction) as it tries to flow out, as shown in Fig. 10.

3.3. Case 3: a water film with a thickness of 0.5 mm placed on the bottom surface of the inlet manifold, without blocking the inlet of each channel of every unit cell

As shown in Fig. 3(c), this simulation was a modification of Case 2. The only change was that the inlet of each channel in every unit cell was not blocked, therefore, air could flow out easier and thus a faster water draining process was expected.

3.3.1. Comparison of Cases 2 and 3

Because the inlet of each channel in every unit cell was not blocked, the initial airflow through each gas flow channel was very strong. Thus, water could sink into the gas flow channels easier than in Case 2. As shown in Fig. 11, water descended into the gas flow channels very fast and at $t = 3$ ms, there was already no liquid water left in the inlet manifold. This was a better situation in terms of PEM fuel cell performance when compared to Case 2. When water was flowing through the gas flow channels, most of it was on the right side of the channel—the leeward side. This was because water entered the gas flow channels from the right side, and due to the wall adhesion effects, it would not be able to easily move to the other side. In contrast to Case 2, the right side gas flow channels had a larger amount of water distribution. This is because there was a large amount of water between the air inlet and the far right side unit cell. In Case 2, this part of the water film kept moving forward without sinking into the gas flow channels significantly. But in this case, because the inlet of each channel in every unit cell was not blocked, stronger airflow would drive this part of the water into the nearest gas flow channels. This was why the right side flow channels had larger water distributions. Generally, this condition is preferred to the one in Case 2. For this kind of water distribution, the gas flow channels further away from the outlet of outflow manifold would have stronger air streams. Differing from Case 2, these air streams would facilitate water to flow out of the manifold than to block them. When water moved into the outflow manifold, small water droplets were formed because the water was broken up by the high velocity airflow. Therefore, this case had the fastest water draining in the present investigation, even when compared to the small amount of water in Case 1.

By comparing the results and flow phenomena in Cases 2 and 3, it could be shown that blocking the inlets of the unit cells could severely decrease the water draining ability of a fuel cell, which is not suitable for fuel cell performance. If all of the flow channels were blocked, as with the initial condition of Case 2, airflow would fragment the water film blocking the gas flow channels first, thus allow air to flow through the gas flow channels. However, the airflow rate would still be very low, so

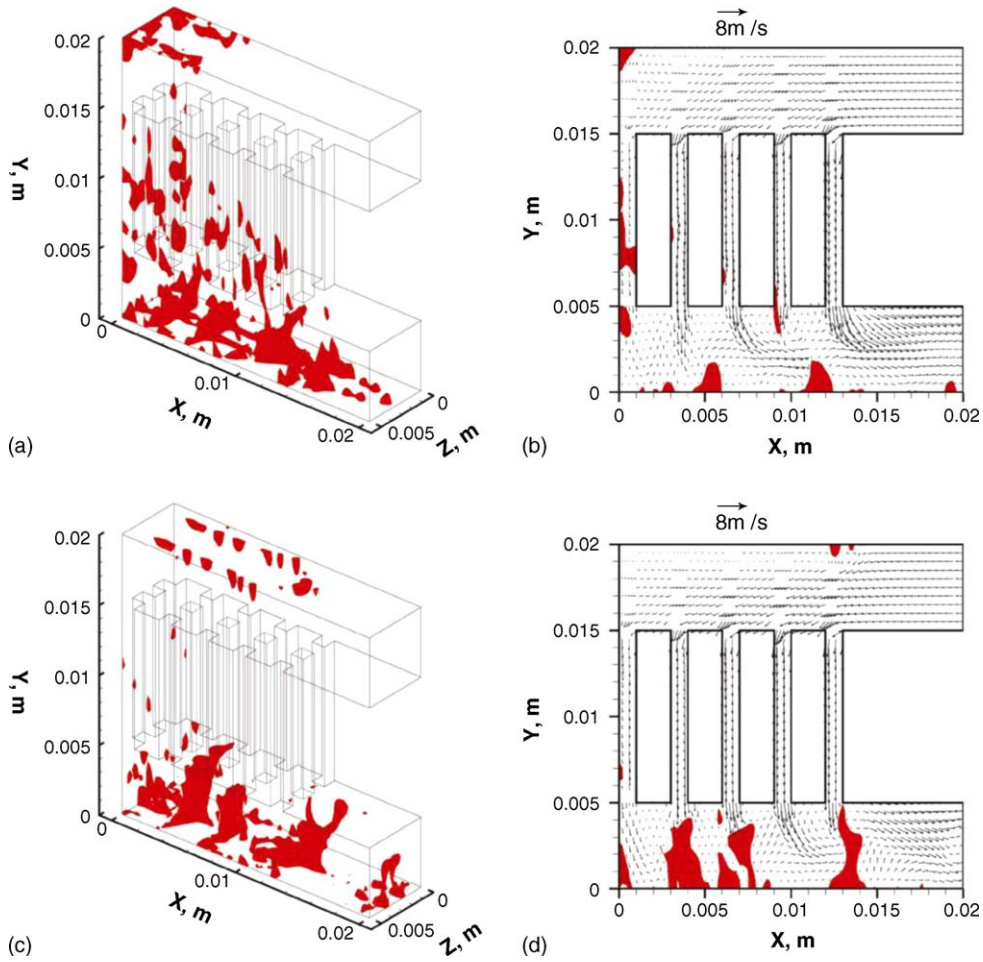

Fig. 10. Water distribution and velocity field in 3D view and on the center-plane of the z-direction: (a) $t = 6$ ms, in 3D view; (b) $t = 6$ ms, on the center-plane of the z-direction ($z = 2.5$ mm); (c) $t = 9$ ms, in 3D view; (d) $t = 9$ ms, on the center-plane of the z-direction ($z = 2.5$ mm).

that the rest of the liquid water in the inlet manifold would not easily move into the gas flow channels. Water would become unevenly distributed in the gas flow channels, and air would flow through the ones with less water distribution. This could explain why the liquid water draining process in Case 2 was slow. However, most of these problems were avoided in Case 3. Because the gas flow channels were not blocked initially, water could flow, very fast, through them. In addition, the airflow rates through all of the gas flow channels were at a high level. This also facilitated the rest of the water to move into the gas flow channels much faster, thus accelerating the water draining process.

3.3.2. Arrangement of the gas flow outlet

By investigating the water flow behaviour in the first three cases, it was also found that the location of the gas flow outlet of the manifold is a very important factor which affected the water draining process. If the gas flow channels further away from the gas flow outlet had greater water distribution, then the water flow out of these channels would be blocked by the air streams from the remaining gas flow channels. This is because the other gas flow channels with relatively smaller water distributions have stronger air streams flowing through them, thus blocking the water further away from the gas flow outlet. The similar conclusion was also drawn in reference [9]. Therefore, no matter what kind of shape of gas flow channels was used, the flow channels closer to the gas flow outlet will always have better water drainage. Better water draining conditions could be achieved when the gas flow channels closest to the gas flow outlet have the largest water distribution, as in Case 3. So the gas flow channels further away from the gas flow outlet would have much stronger air streams, which would facilitate, rather than block, the liquid water to flow out of the manifold. This is a very helpful factor in improving fuel cell performance. Therefore, investigating water flow phenomena in different cells, and choosing the best location for the gas flow outlet of the manifold, could greatly improve fuel cell performance.

3.4. Case 4: water films with a thickness of 0.2 mm placed on the leeward (right) side surface of each gas flow channel in the unit cells

In Case 4, the leeward (right) side surface of each gas flow channel was covered with a water film that has a thickness of 0.2 mm. These surfaces were assumed to be the electrode surfaces of the gas flow channels on the cathode side, on which

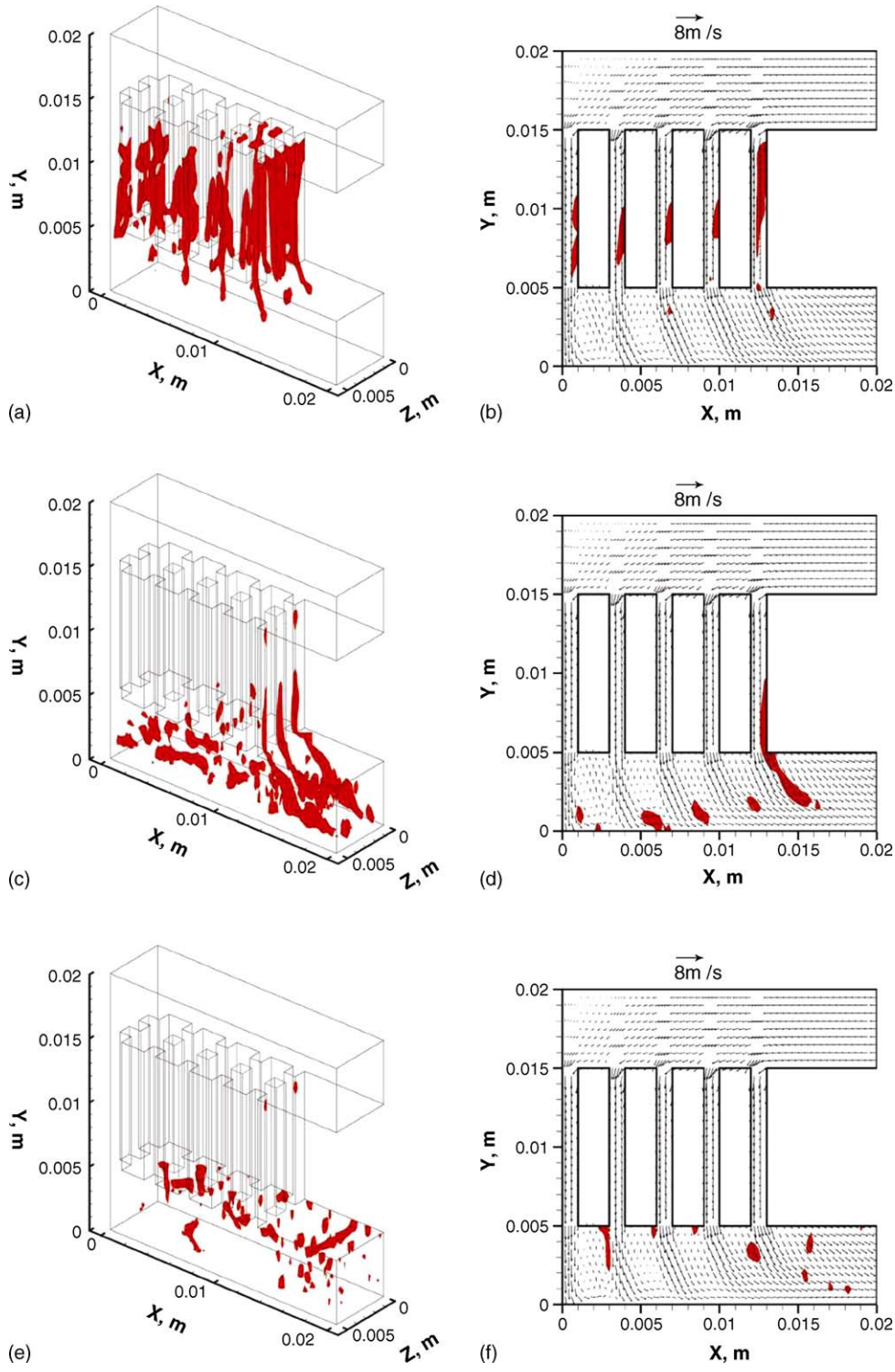

Fig. 11. Water distribution and velocity field in 3D view and on the center-plane of the z-direction: (a) $t = 1.5$ ms, in 3D view; (b) $t = 1.5$ ms, on the center-plane of the z-direction ($z = 2.5$ mm); (c) $t = 3$ ms, in 3D view; (d) $t = 3$ ms, on the center-plane of the z-direction ($z = 2.5$ mm); (e) $t = 4.5$ ms, in 3D view; (f) $t = 4.5$ ms, on the center-plane of the z-direction ($z = 2.5$ mm).

water films could be formed by chemical reactions and condensation during PEM fuel cell operations. Here, the electrochemical reaction is not considered while the water film is used to simulate the water production. The initial water distribution is shown in Fig. 3(d). The ability of water draining was tested, and the velocity field affected by the water distribution was studied.

3.4.1. Water descending and ascending

Water was initially evenly distributed in every gas flow channel. As shown in Fig. 12, in the long run, water started to descend due to the effects of gravity and the dragging force. The amount of water in each gas flow channel was the same, and the airflow rate was evenly distributed. Therefore, water descended with

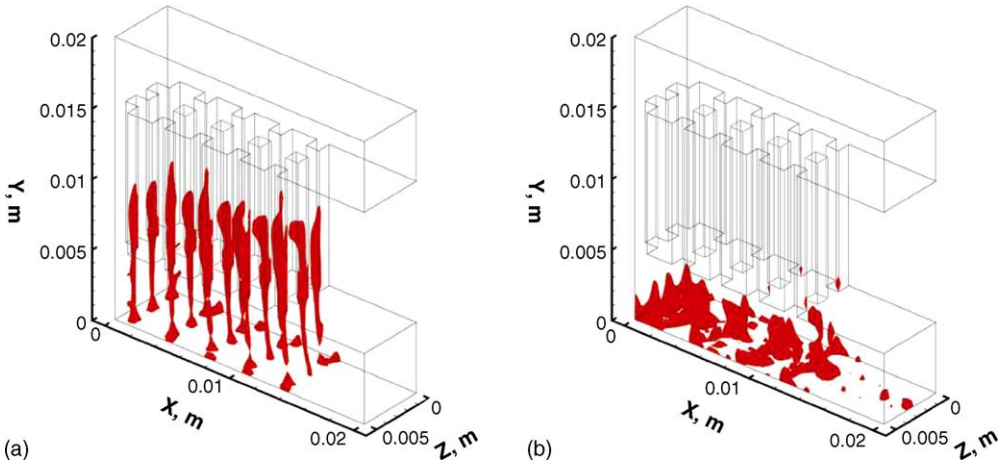

Fig. 12. 3D view of water distribution: (a) $t = 1.5$ ms and (b) $t = 3$ ms.

almost the same velocity and flow behaviour and at $t = 3$ ms, all the water in every gas flow channel had been drained into the outflow manifold.

Fig. 13 shows the velocity field and water distribution on different planes of the z-direction. At $t = 3$ ms, all of the water had moved into the outflow manifold, and there was no water left in the gas flow channels. The velocity field in every gas flow channel was almost the same. At the exits of the gas flow channels, airflow was directed downward (along the negative y-direction) and strong air streams were formed. As mentioned earlier, these strong air streams would block air and water from the left side (the other side of the gas flow outlet of manifold) and were also reflected by the bottom surface of the outflow manifold. Therefore, between every two air streams from the gas flow channels, there would be a velocity field formed directed upward (along the positive y-direction).

Fig. 14 gives a different view at $t = 3$ ms. In the outflow manifold, on the plane crossing the center of the far left unit cell, as shown in Fig. 14(a), airflow was directed downward with a relatively higher velocity. But at the sections between two downward flow streams, as shown in Fig. 14(b and c), air and water were flowing upward with a relatively lower velocity. The air and water were squeezed into those sections by the two strong air streams on either side and since there were two high velocity fields formed on both sides of this section, it was difficult for the air and water to flow out and the path with lowest resistance was upward.

Fig. 15 shows that at a later time, on the plane close to the surface at $x = 0$, water was squeezed and forced to ascend into the gas flow channels, as shown in Fig. 15(b and c). It was found in previous cases that air and water were blocked by stronger air streams, but the water did not ascend into the gas flow channels. Clearly, this indicates a severe problem because the gas flow channels were blocked again. The reason that this kind of flow phenomenon occurred was because the air streams from the gas flow channels were stronger than in the previous cases. In the previous cases, there was always some water left in the gas flow channels or the inlet manifold that could affect the air streams flowing into the outflow manifold. In Case 4, however, water descended from every channel surface at the same time and thus the air streams passing through the gas flow channels met insignificant resistive forces. Ultimately, the squeeze effect was much more severe and the water ascended higher than in the previous cases.

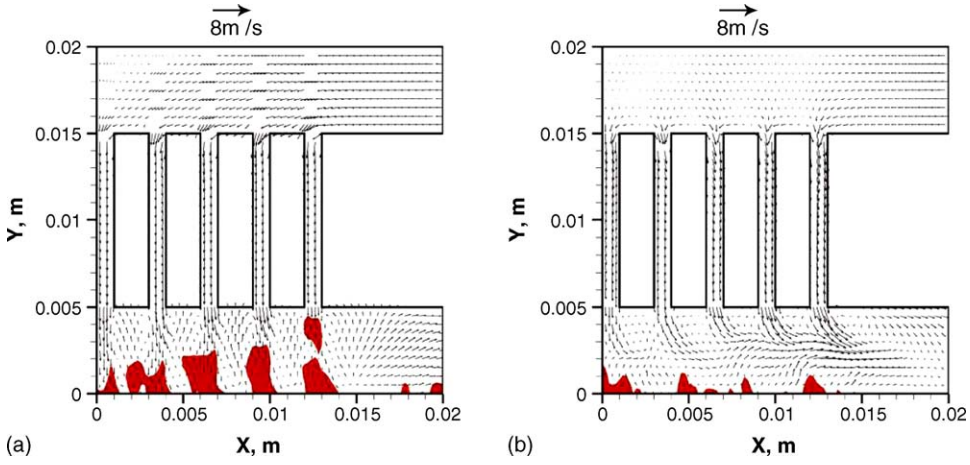

Fig. 13. Water distribution and velocity field in different planes: (a) $t = 3$ ms, on the center-plane of the z-direction ($z = 2.5$ mm) and (b) $t = 3$ ms, on the plane close to $z = 0$.

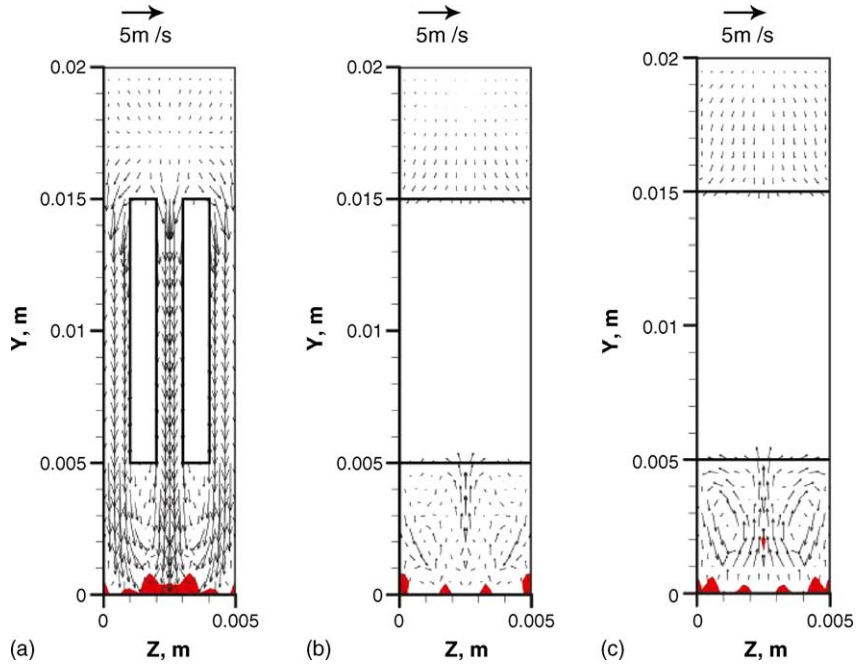

Fig. 14. Water distribution and velocity field on different planes: (a) $t = 3$ ms, on the center-plane crossing the far left cell ($x = 0.5$ mm); (b) $t = 3$ ms, on the plane at $x = 1.5$ mm; (c) $t = 3$ ms, on the plane at $x = 5$ mm.

Fig. 16 shows a plane just between the two far left cells, at $x = 2$ mm. In time, water was pushed upward by a double vortex. Once the water reached the top surface of the outflow manifold (at $y = 0.005$ m), it remained on that surface and eventually moved into gas flow channels.

As shown in Fig. 17, at $t = 2.4$ ms, the right sides of the gas flow channels were blocked by water films, and the air streams flowing out of these gas flow channels were reflected by the water films. Therefore, these reflected air streams descended and moved to the left (along the negative y- and x-directions), as shown. After these air streams flowed into the outflow manifold, they were reflected again by hitting the bottom surface and thus ascended and moved to the left (along the positive y-direction and negative x-direction). In this kind of condition, water was moved further away from the gas flow outlet. This is why some water stuck to the surface at $x = 0$ and ascended, as shown in Fig. 15. But this kind of flow pattern did not last long and at $t = 3$ ms, all the water films were pushed away from the gas flow

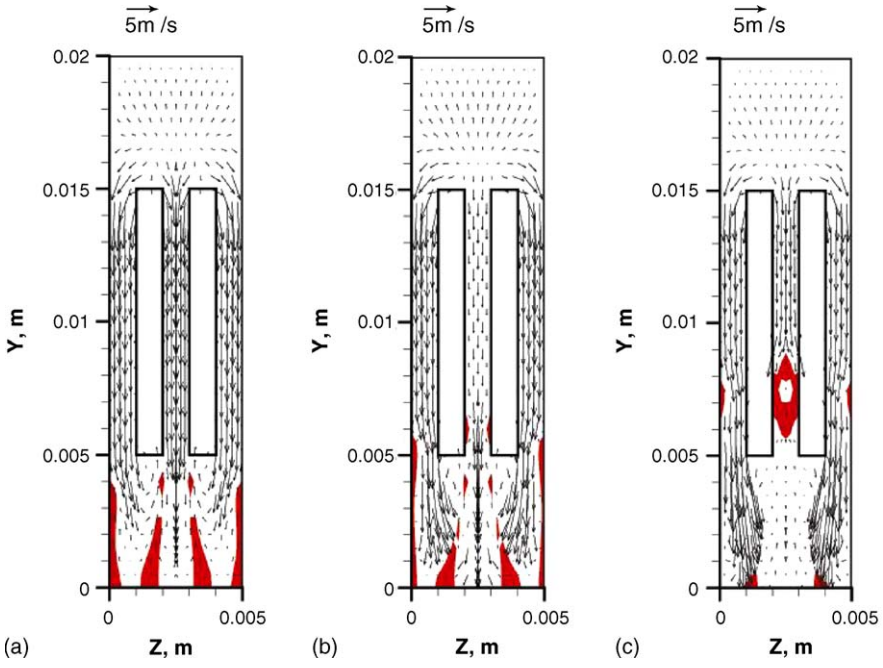

Fig. 15. Water distribution and velocity field on the plane close to $x = 0$: (a) $t = 4.5$ ms; (b) $t = 6$ ms; (c) $t = 9$ ms.

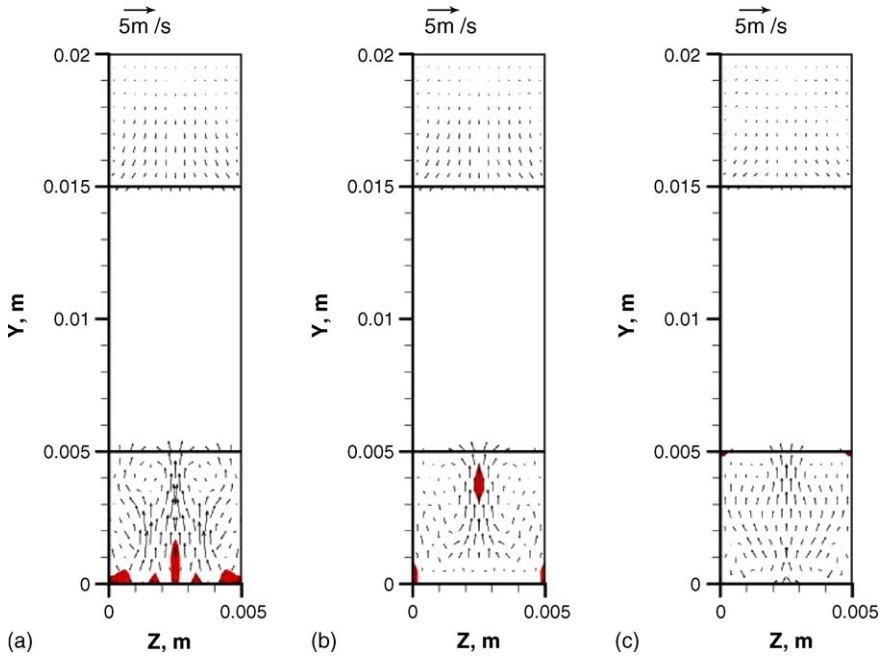

Fig. 16. Water distribution and velocity field on the plane at $x = 2$ mm: (a) $t = 3$ ms; (b) $t = 4.5$ ms; (c) $t = 9$ ms.

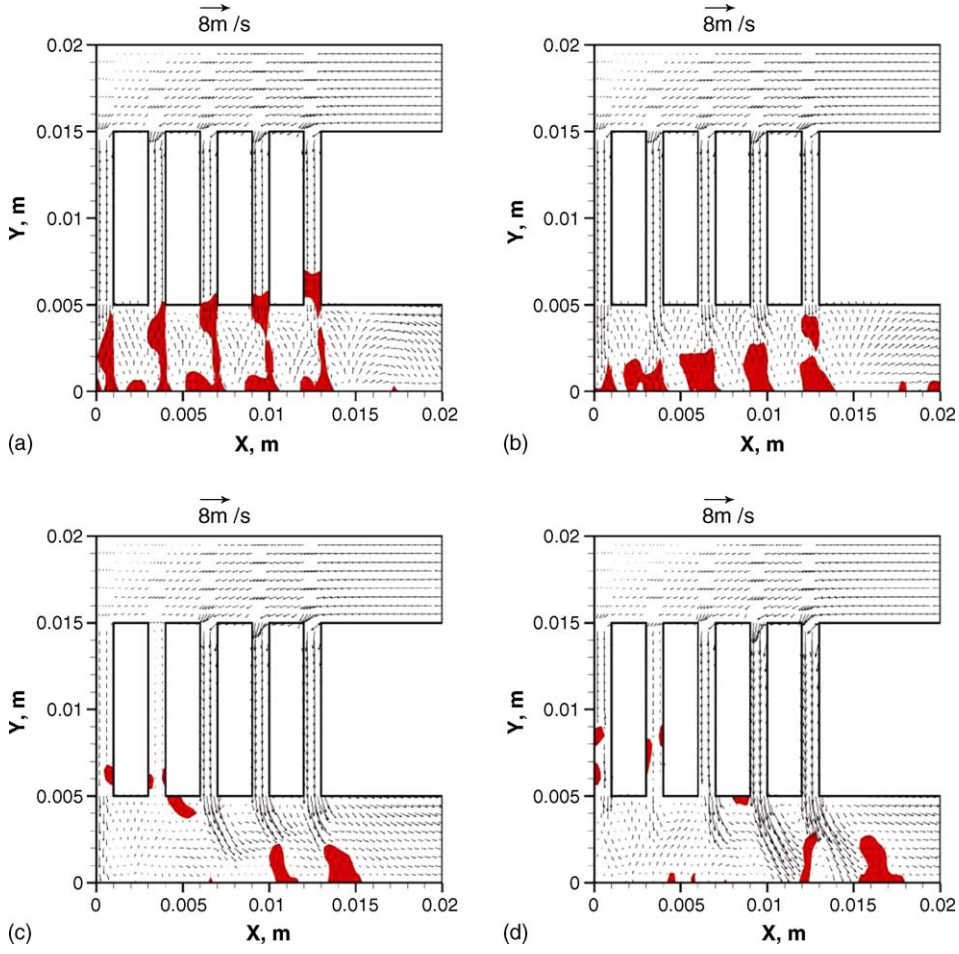

Fig. 17. Water distribution and velocity field on the center-plane of the z-direction ($z = 2.5$ mm): (a) $t = 2.4$ ms; (b) $t = 3$ ms; (c) $t = 6$ ms; (d) $t = 9$ ms.

channels. The air streams from the gas flow channels would no longer be reflected to flow along the negative x-direction. However, there was already some water moved to the left side (along the negative x-direction), especially for the water from the two left cells. After $t = 3$ ms, the water which was initially pushed to the left side (along the negative x-direction) would keep ascending and get into the two far left cells, explaining why the two left cells were blocked with water. As the velocity field in the outflow manifold got closer to the gas flow outlet of the manifold, a larger exiting velocity could be observed in Fig. 17(c and d). At a closer location to the gas flow outlet, there would be less air streams that resist air and water flowing out. For instance, for the far right cell, there were no air streams, which stopped this cell's outgoing air streams from flowing out of the outflow manifold. But the outgoing air and water from the cell second to the right would be blocked by the far right cell's air streams. Generally, the further from the gas flow outlet of the manifold, the greater number of air streams that would block air and water flowing out. As earlier mentioned, this problem was also encountered in the previous cases. This is a common problem that is inevitable for parallel flow channels; however, it could be remedied by modifying the shape of gas flow channels and manifolds. After a while, water ascended to the middle height of the gas flow channels (about $y = 0.01$ m), and after that, it could no longer keep moving upward, as shown in Fig. 17(d), so that water will descend into the outflow manifold again.

3.5. Case 5: water films with a thickness of 0.2 mm placed on the windward (left) side surface of each gas flow channel in the unit cells

Case 5 was simulated to compare with Case 4. In this case, the MEA side was assumed to be windward (on the left-hand side). Therefore, the water films formed due to chemical reactions would also be assumed on this side and the initial water distribution is shown in Fig. 3(e).

3.5.1. Comparison of Cases 4 and 5

Similar to Case 4, as shown in Fig. 18, all of the water films descended into the outflow manifold at the same time. In contrast to Case 4, the air streams from the gas flow channels were reflected another way: downward, but towards the gas flow outlet. This is because the water films in this case were on the other side. These air streams would be reflected again at the bottom surface of the outflow manifold, to ascend and flow out (along the positive y- and x-directions). Therefore, water in the outflow manifold was moved towards the gas flow outlet. This is the major difference between Cases 4 and 5. The water flown away by the two different reflected air streams would block different gas flow channels.

Eventually, water started to ascend from the bottom surface of the outflow manifold. As mentioned earlier, water was initially slightly pushed to the gas flow outlet hence when the water moved upward, the cells on the right side would be blocked and it would keep ascending in the gas flow channels. At $t = 9$ ms, as shown in Fig. 18(e and f), some water even moved into the inlet manifold. The reason why the water moved higher in the gas flow channels than in Case 4 was because there were some reflected air streams that facilitated the water to flow upward. This could be explained with the help of Fig. 18(f), which shows that all the four right cells were blocked with water, and thus most of the air was flowing through the far left cell. As a result, very strong air stream was flowing out of the far left gas flow channel and was also reflected by the bottom surface of the outflow manifold. Therefore, there was a velocity field flowing up under the four right side cells, which helped the water in the gas flow channels to keep ascending. But in Case 4, as earlier mentioned, the two left cells were blocked with water and most of the air was passing through the right side cells, and these air streams were also reflected by the bottom surface of the outflow manifold. Nevertheless, they were reflected to flow out of the manifold, and thus would not facilitate the ascent of water in the two left cells. This phenomenon is shown in Fig. 17, and this is why the water flowed much higher than in Case 4.

It took a longer time for all the water to be drained in Case 5 than Case 4. Also in Case 5, water even moved into the inlet manifold, thus delaying the water draining process. Clearly, it is not a good phenomenon because the gas flow channels were blocked severely. Water in Case 4 only blocked two cells, and its ascent was not much. As was concluded in Cases 2 and 3, arranging the flow channels which may have a greater amount of water distribution close to the gas flow outlet would greatly improve fuel cell performance. This conclusion could also be extended thus; positioning the MEA side of the fuel cell close to the gas flow outlet would also greatly improve fuel cell performance. But Case 4 was still not a suitable condition for proper and efficient fuel cell operation; this is because the water still moved upward into the gas flow channels. One way to avoid this kind of problem is to optimize the shape of the flow channels and manifolds. In both Cases 4 and 5, water was flown up by reflected air streams from the gas flow channels. Remedying these air stream reflection effects is the key to fixing this kind of problem. The easiest way to solve it is simply to make the outflow manifold higher (expand the outflow manifold along the y-direction). With a larger outflow manifold, air streams from the gas flow channels would have more space to move in. This would greatly remedy the reflection effects, thus solving the upward flowing water problem.

3.5.2. Comparison of straight and serpentine [9] gas flow channels

In reference [9], similar study by arranging the MEA side to be windward and leeward was also carried out, it was also concluded that arranging the MEA to be closer to the gas flow outlet is a better design in terms of water drainage. Therefore, the conclusion could be extended here that, regardless of the patterns of the gas flow channels (straight or serpentine), arranging the MEA side closer to the gas flow outlet is a better for faster water drainage. It is noteworthy to mention that for a serpentine-type of design water cannot flow back into the gas flow channels, which was observed in [9], while for straight-type of design described here water can flow back into the gas flow channels. Therefore, a better drainage could be achieved with serpentine gas flow channels, although which are more complex and expensive.

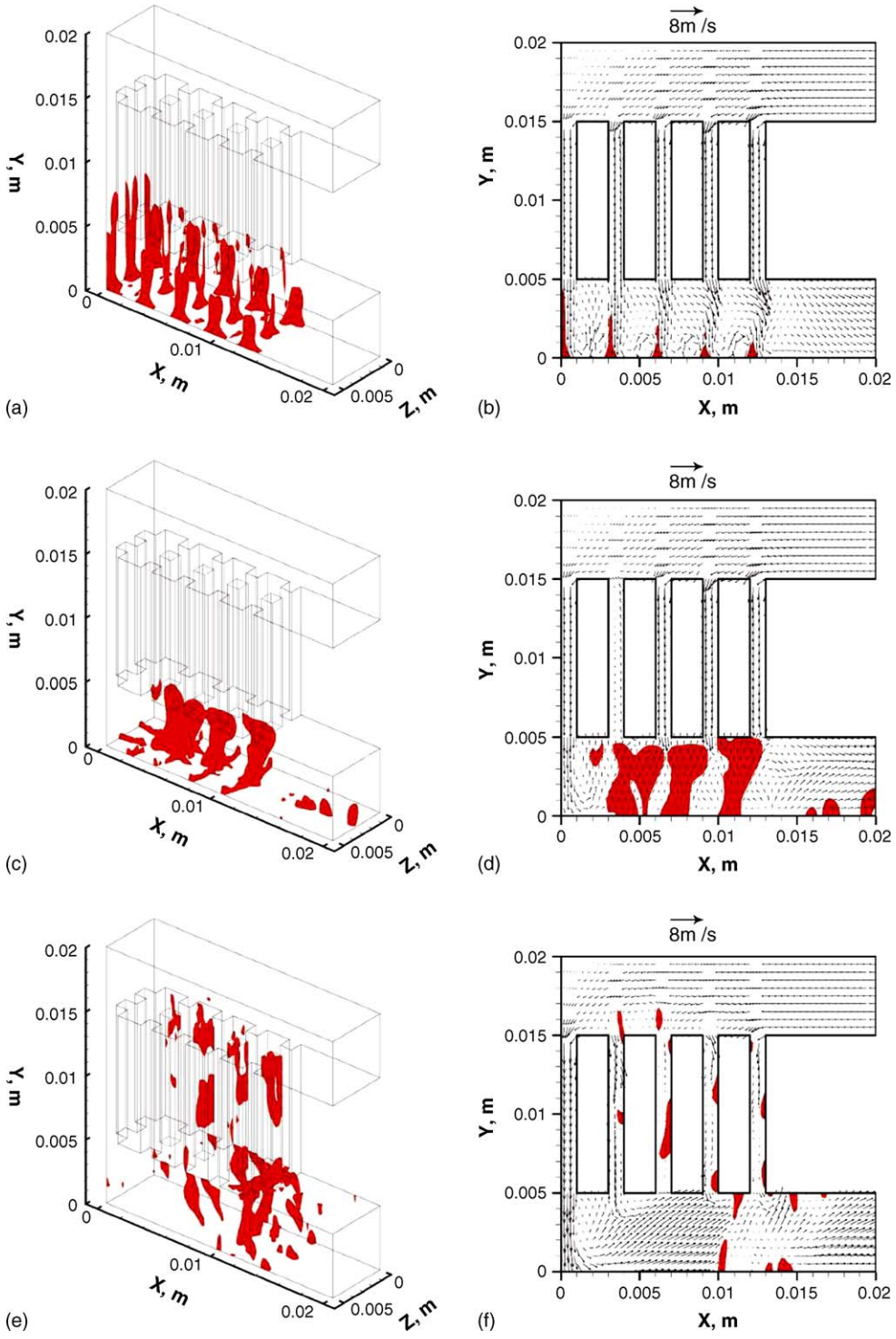

Fig. 18. Water distribution and velocity field in 3D view and on the center-plane of the z-direction: (a) $t = 1.5$ ms, in 3D view; (b) $t = 1.5$ ms, on the center-plane of the z-direction ($z = 2.5$ mm); (c) $t = 3$ ms, in 3D view; (d) $t = 3$ ms, on the center-plane of the z-direction ($z = 2.5$ mm); (e) $t = 9$ ms, in 3D view; (f) $t = 9$ ms, on the center-plane of the z-direction ($z = 2.5$ mm).

3.6. Case 6: water films with a thickness of 0.5 mm attached to the surrounding walls near the manifold inlet

Case 6 was simulated to consider wall adhesion, water gravity and air dragging effects. It was assumed that water was condensed or supplied on the surrounding surfaces of the inlet manifold. Four water films with thicknesses of 0.5 mm were attached to the surrounding walls, as shown in Fig. 3(f). All the water films were 5 mm long. Since there was a large amount of water which stuck on the surrounding walls, wall adhesion and gravity were expected to affect water movement significantly.

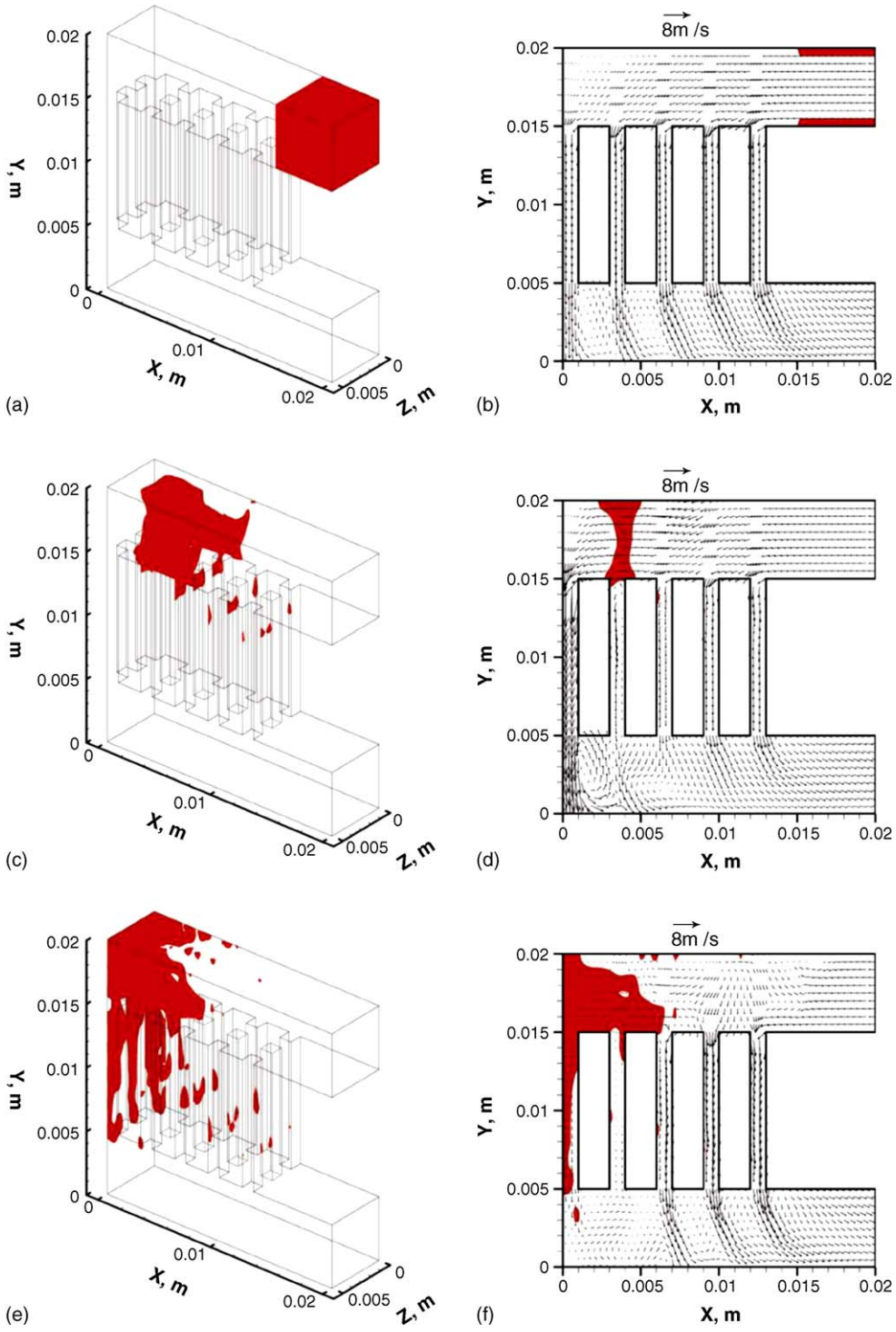

Fig. 19. Water distribution and velocity fields in 3D view and on the center-plane of the z-direction: (a) $t = 0$, in 3D view; (b) $t = 0$, on the center-plane of the z-direction ($z = 2.5$ mm); (c) $t = 3$ ms, in 3D view; (d) $t = 3$ ms, on the center-plane of the z-direction ($z = 2.5$ mm); (e) $t = 6$ ms, in 3D view; (f) $t = 6$ ms, on the center-plane of the z-direction ($z = 2.5$ mm).

3.6.1. Large amount of water transport in the inlet manifold

Water did not sink into the gas flow channels that much as it first moved through the inlet manifold, as shown in Fig. 19. At $t = 3$ ms, water had already passed over the inlets of the two cells near the inlet, with only a small amount descending in the cells. Therefore, gravity effects were still not significant when compared to air dragging forces, even though the amount of water was large. On the center-plane of the z-direction, water was just above the second left cell, and airflow through this cell was much less than the far left one. As was concluded in Case 1, even if there was only a small amount of water left

in the gas flow channels, airflow would be blocked severely. Unexpectedly, gravity was still not significant in this case, not only because water was moving too fast, but also because there was wall adhesion preventing water from descending. The wall adhesion effect is not suitable because the large amount of water would keep going until it hits the wall at $x = 0$. This would cause the first left channel to be severely blocked. In due course, water would keep moving forward, as shown in Fig. 19(e and f). At $t = 6$ ms, the far left cell was almost full of water, and there was also a large amount of water flow backward to the air inlet. This "flowing back" phenomenon was also observed in Cases 1 and 2. By comparing these three cases, the authors concluded that once there is water hitting the wall at $x = 0$, there would be some amount of water flowing up to the top surface of the inlet manifold, which would move back to the airflow inlet. This is the phenomenon that most researchers have spent tireless efforts in trying to avoid because when water is continuously condensed in practical applications, the inlet manifold would continue to be filled with water. One important reason why water would flow back is because there was a vortex in the top left corner of the inlet manifold. This vortex formed because airflow reflected after it hits the wall at $x = 0$, thereby forcing the water to flow backward. The other reason is that the airflow was fully developed, and the airflow velocity around the surrounding walls of the inlet manifold was relatively low, hence there would not be enough resistance to stop the water from moving backward. To reduce the airflow reflection effect from the wall at $x = 0$ and make the airflow velocity higher around the surrounding walls of the inlet manifold, two solutions are proposed by the authors. The airflow reflection effect could be reduced by curving the wall at $x = 0$. This means curving the top left corner of the inlet manifold thus airflow would be directed to flow along the walls and the reflection effects would be reduced. The top surface of the inlet manifold could also be modified to increase the airflow velocity, for instance, by use of an inclined top surface. This means that there would be a large cross-section at the airflow inlet, but the height of the inlet flow manifold would decrease along the negative x-direction. Therefore, on the other side of the inlet manifold ($x = 0$), the height of the inlet manifold would be a minimum and the decrease of inlet manifold height would theoretically increase the airflow velocity, thus preventing water from flowing backward. In reference [9], a similar issue was also addressed.

4. Conclusions

A 3D, straight micro-parallel-channels with inlet and outlet manifolds for PEM fuel cell stack cathode has been simulated by the volume of fluid two-phase flow model under different initial water distributions. By investigating the flow behaviour of the liquid water and the airflow velocity fields, the following water management issues have been concluded:

1. For a design with straight-channels, water in the outflow manifold could be easily blocked by air/water streams from the gas flow channels. This would slow down the water draining process. With water continuously flowing into the outflow manifold, the outflow manifold may be blocked by this increasing amount of water. As discussed in the author's previous research, the serpentine design would improve such situation.
2. For designs with either straight or serpentine channels, the airflow could be severely blocked even if there was only a small amount of water in the gas flow channels, thus causing airflow to be unevenly distributed. This could severely decrease fuel cell performance. The serpentine design could provide a powerful water removal characteristic, "collecting and separating water" by the U-turns.
3. For designs with either straight or serpentine channels, if water hits the wall that faces the air inlet of the inlet manifold, water could be moved back to the air inlet again. In this case, water could not be moved into the gas flow channels on time, and the inlet manifold may become blocked with continuously supplied water. An inlet manifold with gradually reduced cross-section area and an outlet manifold with gradually increased cross-section area have been proposed to resolve this challenge.
4. Keeping a unit cell that may have the largest amount of water close to the outlet of the outflow manifold could greatly improve fuel cell performance; therefore, a design where the outlet stream exit has the same direction of inlet stream in the inlet manifold would be a better design for either straight- or serpentine-type of designs.
5. Keeping the MEA side of the gas flow channels close to the outlet of the outflow manifold is recommended to improve the water draining process, thus improving fuel cell performance for either straight- or serpentine-type of designs.
6. A curved wall, which faces the airflow inlet could prevent water from flowing back to the air inlet again, allowing water to be moved into the gas flow channels faster for either straight- or serpentine-type of designs.
7. Wall adhesion effects could slow down the water draining process, thus reducing the fuel cell performance. Thus, selecting the materials with less water wall adhesion effect to construct the cathode channels would assist the water removal process.

Acknowledgements

The authors are grateful for the support of this work by the Auto21 Networks of Center of Excellence Grant D07-DFC, the Natural Sciences and Engineering Research Council of Canada (NSERC) and the Graduate School at the University of Windsor.

References

[1] J. Larminie, A. Dicks, Fuel Cell Systems Explained, second ed., John Wiley & Sons, New York, 2000.
[2] J.S. Yi, J.D. Yang, C. King, AIChE J. 50 (2004) 2594.
[3] S. Dutta, S. Shimpalee, J.W. Van Zee, J. Appl. Electrochem. 30 (2000) 135.
[4] E. Hontanon, M.J. Escudero, C. Bautista, P.L. Garcia-Ybarra, L. Daza, J. Power Sources 86 (2000) 363.

[5] S.W. Cha, R. O'Hayre, Y. Saito, F.B. Prinz, J. Power Sources 134 (2004) 57.
[6] A.A. Kulikovsky, Electrochem. Commun. 3 (2001) 460.
[7] L. You, H. Liu, Int. J. Heat Mass Transfer 45 (2002) 2277.
[8] P. Quan, B. Zhou, A. Sobiesiak, Z. Liu, Water behavior in serpentine micro-channel for proton exchange membrane fuel cell cathode, J. Power Sources 152 (2005) 131.
[9] K. Jiao, B. Zhou, P. Quan, Liquid water transport in parallel serpentine channels with manifolds on cathode side of a PEM fuel cell stack, J. Power Sources 154 (2006) 124–137.
[10] Fluent 6.1 User's Guide, Fluent Inc.
[11] J.U. Brackbill, D.B. Kothe, C. Zemach, J. Comput. Phys. 100 (1992) 335.